ACS Medicinal Chemistry Letters

Open Access
This article is licensed under CC-BY-NC-ND 4.0

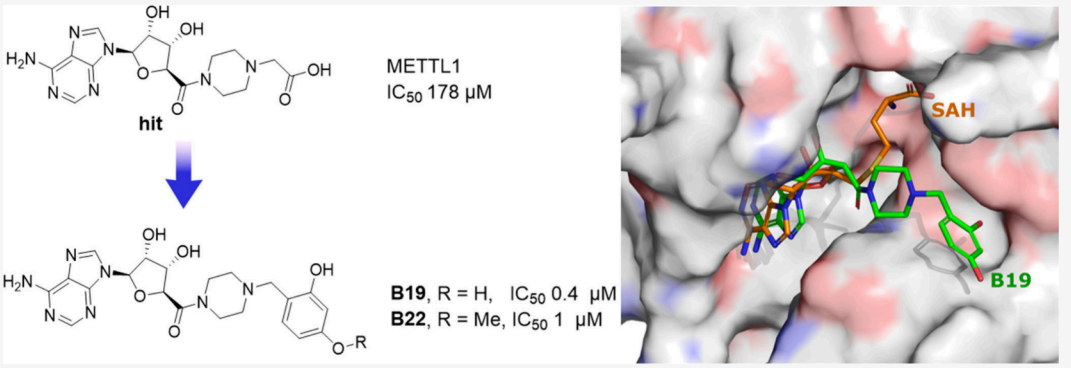
pubs.acs.org/acsmedchemlett
Letter

Adenosine 5′-Carboxamide-Based Inhibitors of METTL1

Olga Bobileva,* Francesco Nai, Sandija Niedrite, Lidia Mayordomo Soler, Irena Leite, and Amedeo Caflisch*

Cite This: ACS Med. Chem. Lett. 2026, 17, 1941−1947
Read Online

ACCESS | Metrics & More | Article Recommendations | Supporting Information



ABSTRACT: METTL1 is the human RNA methyltransferase that catalyzes the methylation of *N*7-guanosine in RNA. Overexpression of METTL1 has been linked to cancer, and increasing evidence supports the therapeutic potential of METTL1 inhibition in oncology. In this study, we have optimized a series of adenosine 5′-carboxamide derivatives as METTL1 inhibitors through structure-guided modifications of a previously discovered hit compound. The advanced inhibitor **B22** shows an IC_{50} of 1 μM in an enzymatic assay, which is a 178-fold improvement with respect to the initial hit. The crystal structure of the des-methyl analogue of **B22** (compound **B19**, IC_{50} = 0.4 μM) provides evidence that the benzylpiperazine moiety is accommodated within the guanosine-binding subsite of METTL1. The inhibitor **B22** shows high solubility and metabolic stability and is selective against a panel of seven histone methyltransferases and the RNA-methyltransferase METTL3/METTL14.

KEYWORDS: *N7-guanosine, epitranscriptomics, methyltransferase, docking, drug discovery*

RNA modification is a significant process for gene regulation. Methyltransferase-like proteins (METTLs) constitute a family of epitranscriptomic writers that serve as key regulators of RNA post-transcriptional modifications.[1] METTL1 in complex with WD repeat domain 4 (WDR4) catalyzes internal methylation at the *N*7 position of guanosine (m7G) in tRNAs, miRNAs, and mRNAs.[2,3] METTL1 utilizes the cofactor *S*-adenosyl-methionine (SAM) as a methyl group donor, converting SAM to *S*-adenosyl homocysteine (SAH). m7G modifications of RNA regulate translation, cell cycle progression, stem cell maintenance, differentiation, and cell migration.[4]

Multiple studies have demonstrated the connection between the overexpression of METTL1/WDR4 and tumorigenesis. tRNA m7G modification deposited by METTL1/WDR4 is upregulated in several cancer types.[5] Increasing evidence suggests that elevated METTL1 expression promotes cancer cell proliferation, migration, and invasion, implicating METTL1 in cancer development.[6−9]

Knockdown of METTL1 or WDR4 reduces m7G modification in tRNAs across several cancer types and exhibits context-dependent effects. For example, knockdown of METTL1 in intrahepatic cholangiocarcinoma suppresses cell migration and invasion, reduces cell growth, and impairs colony-forming ability.[10] In prostate cancer preclinical models, METTL1 knockdown increases intratumoral infiltration of pro-inflammatory immune cells and enhances responses to immunotherapy.[11] METTL1 knockdown suppresses proliferation in lung cancer cells and suppresses both proliferation and migration in bladder cancer cells *in vitro*.[12,13] METTL1 was also linked to anticancer drug sensitivity.[14] Although METTL1 is upregulated and acts as an oncogene in most researched cancer types, METTL1 is a tumor suppressor in breast cancer, and its knockdown promotes breast cancer progression.[15] There is also evidence that METTL1 has oncogene activity independent of its methyltransferase activity. METTL1 promotes sarcomagenesis by increasing tRNA aminoacylation, elevating protein synthesis,

Received: April 10, 2026
Revised: June 15, 2026
Accepted: August 3, 2026
Published: August 10, 2026



ACS Publications
© 2026 The Authors. Published by American Chemical Society

https://doi.org/10.1021/acsmedchemlett.6c00203
ACS Med. Chem. Lett. 2026, 17, 1941−1947

Downloaded from pubs.acs.org/amclct/article-pdf/17/9/1941/6469063/acsmedchemlett.6c00203.pdf by guest on 06 November 2026

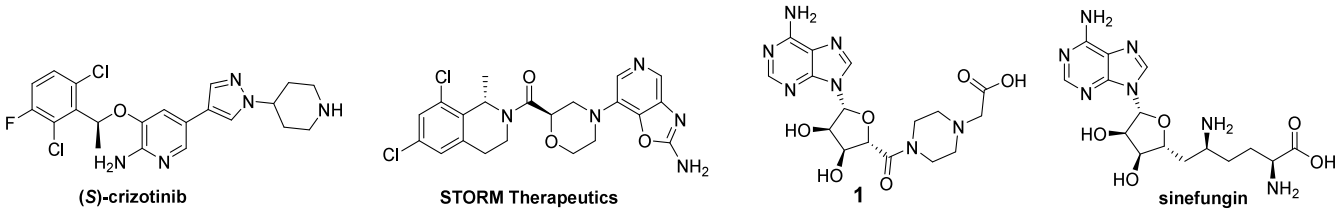
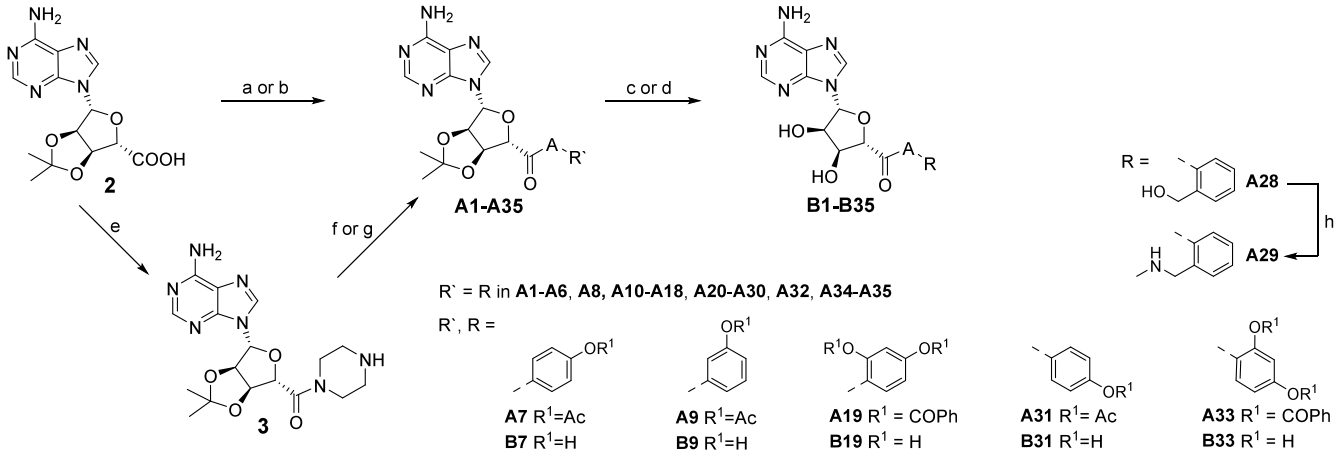


Figure 1. Structures of known METTL1 inhibitors.

Scheme 1. General Synthesis of Target Compounds B1−B35[a]



[a]Reagents and conditions: (a) appropriate amine, HBTU, TEA, DMF, 18 h, rt; (b) appropriate amine, T3P, TEA, EtOAc−DMF, 6−18 h, rt; (c) 50% HCOOH, 6−10 h, 50 °C.; (d) (i) K_2CO_3, MeOH; (ii) 50% HCOOH, 6−10 h, 50 °C.; (e) (i) Cbz-piperazine, T3P, TEA, EtOAc−DMF, 6−18 h, rt; (ii) H_2, 10% Pd/C, MeOH, 4 h, rt; (f) appropriate aldehyde, $Na(OAc)_3BH$, DCE, rt, 16 h; (g) appropriate benzylbromide, TEA, MeCN, 2 h, rt; (h) (i) Dess−Martin reagent, DCM, 18 h, rt; (ii) $MeNH_2HCl$, TEA, $Na(OAc)_3BH$, DCE, 16 h, rt.

and promoting tumor cell growth.[16] Recently, METTL1 was shown to promote leukemia stem cell homeostasis and leukemogenesis via activation of $tRNA^{Phe}_{GAA}$/HCK/CXCR4 signaling.[17] In the same study, it was shown that inhibition of METTL1 by a small molecule eliminates leukemia stem cells and myeloid leukemia.

The number of epitranscriptomic targets currently under active investigation in drug discovery is minimal.[18] The anticancer medication (*S*)-crizotinib (Figure 1) was identified as a METTL1 inhibitor in high-throughput drug screening using the newly developed fluorescent RNA-methyltransferase probe Cy5TAD.[19] A recent patent disclosed a series of dihydroisoquinolinyl-morpholine derivatives with reported low-nanomolar biochemical potency against METTL1.[20] We have identified 11 METTL1 inhibitors representing three distinct chemotypes, with inhibitory potencies ranging from 40 to 300 μM. Among these, the adenine derivative **1** (Figure 1) demonstrated favorable ligand efficiency.[21]

Given its involvement in multiple types of cancer, METTL1 is a compelling target for drug discovery.[22] Here, we report the protein structure-based development of adenosine-containing METTL1 inhibitors using a SAM-mimicking strategy. METTL1 utilizes SAM as a methyl donor, converting it to SAH within the same catalytic pocket. Our molecules are designed to act as SAM-competitive inhibitors to block the co-substrate/co-product binding site.

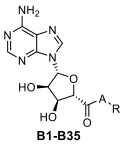
The target compounds were prepared according to the route described in Scheme 1. The synthesis started from 2′,3′-*O*-isopropylideneadenosine-5′-carboxylic acid **2**.[23] Most of the compounds were obtained via amide bond formation using HBTU (**A1−A3**, **A7**, **A8**) or T3P (**A4−A6**, **A9−A21**, **A30−A35**) as a coupling reagent and an appropriate commercially available or synthetically easily accessible amine. Alternatively, we used reductive amination of piperazine **3** with the corresponding benzaldehydes to obtain compounds **A22−A27**. Piperazine derivative **A28** was synthesized using the alkylation reaction of **3** with 2-(hydroxymethyl)benzyl bromide. The benzyl alcohol group of **A28** was oxidized with Dess−Martin periodinane to yield the corresponding benzaldehyde derivative, which we subsequently subjected to reductive amination reaction with methylamine to obtain **A29**. Acetyl or benzoyl phenol protecting groups were removed with potassium carbonate in MeOH. The isopropylidene protecting group was cleaved by treatment with 50% formic acid, yielding the final compounds **B1−B35**.

We selected the previously characterized METTL1 inhibitor **1** (Table 1), which incorporates an adenosine-privileged scaffold, as the starting point for the development of new inhibitors. Piperazine derivative **1** is selective against METTL3/14 and METTL16.[21] The initial design is based on a substitution of the polar carboxylic group of **1** with a less polar group such as phenyl or heteroaryl. It was hypothesized that the phenyl group would occupy the methionine-binding subsite of the SAM pocket or target the RNA-binding site. The IC_{50} value was determined using a luminescence-based METTL1-WDR4 enzymatic assay. Inhibitory activities of the new compounds were evaluated in comparison to sinefungin (Figure 1). To rule out potential assay interference, selected compounds were tested against the downstream reaction and detection components of the assay. No interference was observed (Figure S4).

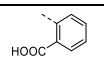
Downloaded from pubs.acs.org/amclct/article-pdf/17/9/1941/6469063/acsmedchemlett.6c00203.pdf by guest on 06 November 2026

https://doi.org/10.1021/acsmedchemlett.6c00203
ACS Med. Chem. Lett. 2026, 17, 1941−1947

Table 1. Chemical Structures and METTL1 Inhibitory Activity of Compounds 1 and B1−B36



B1-B35

Cpd.	A	R	IC_{50}, μM[a]	250 μM, %[b]	100 μM, %[b]	Cpd.	A	R	IC_{50}, μM[a]	250 μM, %[b]	100 μM, %[b]
	Sinefungin		10 ± 2 (*n*=6)			**B18**			n.d.	36	
1			178[c]			**B19**			0.4 ± 0.1 (*n*=4)	14	
B1			46 ± 3 (*n*=3)			**B20**			117 129 (*n*=2)	34	
B2			35 ± 10 (*n*=3)			**B21**			9 8 (*n*=2)	0	8
B3			7 ± 2 (*n*=3)			**B22**			1 ± 0.4 (*n*=3)	1	1
B4			19 ± 1 (*n*=3)	1		**B23**			15 16 (*n*=2)	7	20
B5			n.d.	45		**B24**			59 49 (*n*=2)	12	31
B6			n.d.	72		**B25**			15 19 (*n*=2)	20	22
B7			15 ± 1 (*n*=3)			**B26**			25 26 (*n*=2)	12	17
B8			6 ± 4 (*n*=4)	-6		**B27**			n.d.	45	77
B9			22 27 (*n*=2)	22		**B28**			n.d.	45	65
B10			38 33 (*n*=2)	39		**B29**			n.d.	47	77
B11			16 ± 7 (*n*=3)	1		**B30**			61 36 (*n*=2)	45	
B12			49 ± 5 (*n*=3)	24		**B31**			n.d.	89	
B13			49 52 (*n*=2)	15		**B32**			14 13 (*n*=2)	-3	
B14			n.d.	52		**B33**			100 108 (*n*=2)	29	
B15			15 15 (*n*=2)	5		**B34**			15 12 (*n*=2)	1	
B16			45 28 (*n*=2)	3		**B35**			44 46 (*n*=2)	8	
B17			92 94 (*n*=2)	27		**B36**			n.d.		118

[a]Luminescence-based METTL1-WDR4 enzymatic assay. Data are the mean ± SD calculated from at least three experiments or values of two independent replicates. Number of replicates (*n*) is indicated in parentheses. All curves are shown in Figure S3. [b]Single-dose experiment showing protein residual signal at respective compound concentrations. [c]Data from ref 21. n.d., not determined. The Green color highlights inhibitors with $IC_{50} \leq 1$ μM. Pale green highlights compounds with activity comparable to sinefungin, i.e., IC_{50} in the range 5−20 μM. Yellow indicates compounds with IC_{50} of 25−100 μM. Red indicates compounds with IC_{50} of >100 μM or n.d.

The replacement of the carboxylic acid with the amide analogue **B1** showed a 4-fold increase in activity, while compounds **B2**−**B4** with phenyl or heteroaryl groups directly attached to the piperazine demonstrated more than 5-fold improvement compared to inhibitor **1** (Table 1).

https://doi.org/10.1021/acsmedchemlett.6c00203
ACS Med. Chem. Lett. 2026, 17, 1941−1947

Downloaded from pubs.acs.org/amclct/article-pdf/17/9/1941/6646963/acsmedchemlett.6c00203.pdf by guest on 06 November 2026

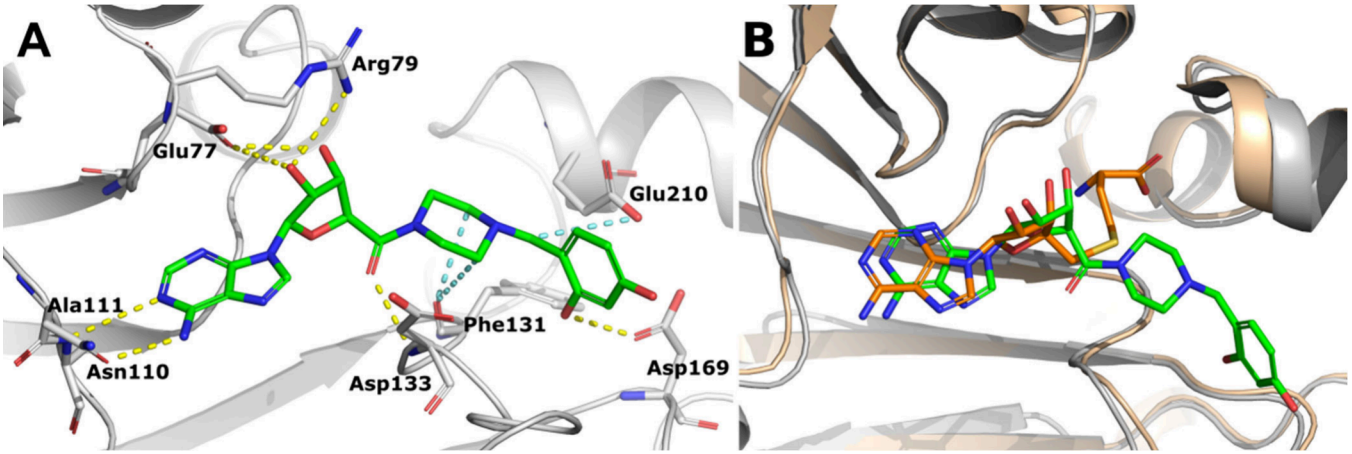


Figure 2. Crystal structure (PDB code 29GE) of the complex of METTL1 (gray) and **B19** (carbon atoms in green). (A) The hydrogen bonds (yellow) and interactions of the positively charged amine of the piperazine (cyan) are emphasized. (B) Superimposed crystal structures of the complex of METTL1 (gray) with **B19** (green), and METTL1 (gold) with SAH (orange, PDB code 7OGJ).

On the basis of these results, a spacer was introduced between the piperazine and benzene ring of the molecule, resulting in sulfonamide **B5** and amide **B6**. However, these modifications led to decreased inhibitory activity compared with compound **B4**. In contrast, the methylene-spaced 4-hydroxybenzyl containing **B7** is twice as active as its shorter analogue **B2**. Subsequently, we decided to explore the role of substituents on the benzyl group of piperazine. A set of functional groups with contrasting electronic properties as well as moieties acting as hydrogen-bond donors (e.g., OH, NH_2) or hydrogen bond acceptors (e.g., COOMe) were introduced to probe the nature of the binding pocket, resulting in a series of benzyl piperazine analogs **B7**-**B29**.

In this series, we obtained several compounds with inhibitory activities comparable to sinefungin (within ±2-fold of its IC_{50} of 10 μM, pale green in Table 1) and two compounds, **B19** and **B22**, that are an order of magnitude more potent than sinefungin. Most of these compounds bear a hydroxyl group or other hydrogen-bond donor group at the *ortho* or *para* position of the benzyl group, except for **B15**, where 4-NO_2 is a weak hydrogen bond acceptor. Compound **B19** is 445-fold more potent than its parent compound **1**. The thermal shift assay of the compound **B19** with both METTL1 and METTL1/WDR4 showed that **B19** stabilizes the protein (Figure S1).

We determined the crystal structure of METTL1 in complex with **B19**. Crystal structure data are provided in Table S1. The structure reveals a conserved binding mode of the adenosine moiety (Figure 2). The adenine forms hydrogen bonds with the backbone NH group of Ala111 and with the side chain of Asn110. The ribose hydroxyl groups form hydrogen bonds with Glu77 and Arg79. The carbonyl group interacts with the backbone NH of Asp133. The piperazine is positively charged at physiological pH (the predicted pK_a of *N*-methylpiperazine is about 9.0), and thus its tertiary amine is involved in favorable electrostatic interactions with the carbonyl of Phe131 and the side chain of Glu210 (cyan dotted lines in Figure 2A). The dihydroxybenzyl group of **B19** extends toward the RNA-binding site. The 2-hydroxy group acts as a hydrogen bond donor to the side chain of Asp169, providing a favorable electrostatic interaction that contributes to the high affinity of **B19**.

To understand the structural basis for the structure−activity observations for the compounds **B1**−**B29**, we performed a docking study using the crystal structure of METTL1 in complex with compound **B19**. The docking models of compounds **B7**−**B11**, **B15**, and **B21** indicated that these molecules adopt positions similar to those of **B19**. The *p*-hydroxy group of **B7** binds to Asp169 with a slightly shifted position of piperazine. Additionally, phenol forms a hydrogen bond with Thr168 (Figure 3). The *m*-hydroxy group of **B9**

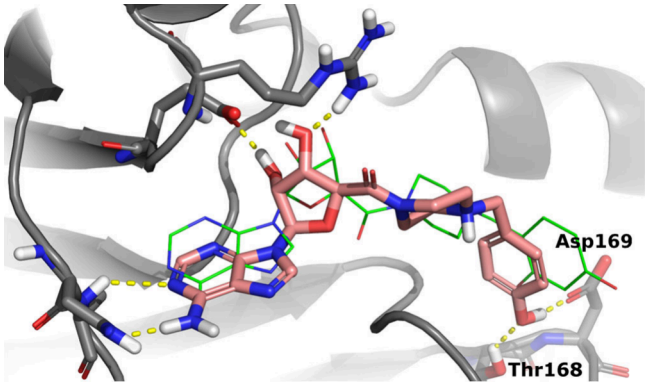


Figure 3. Docked pose of compound **B7** in METTL1. The crystal structure (PDB code 29GE) of the complex of **B19** (carbon atoms in green) and METTL1 (ribbon model, carbon atoms of side chains in gray) was used for docking.

(Figure S2B) and the methylaniline NH of **B21** interact with Asp169 similarly. The high potency of **B3** could be explained by the hydrogen bond between the protonated pyridine of **B3** and Asp169 (Figure S2A). The heterocyclic NH in the pyrrolopyridine of **B11** acts as a hydrogen-bond donor (Figure S2C). It serves as a phenol bioisostere, like indoles, which are reported phenol bioisosteres.[24]

Compound **B15** exhibits strong inhibitory activity despite lacking hydrogen-bond donors at the benzyl group. This activity can be explained by the interaction of its *p*-nitro group and Glu210 by the formation of a salt bridge (Figure S2D).

The activity of compounds containing 2-hydroxy group is strongly influenced by additional substituents at the benzyl group. No clear correlation was observed between the acidity of the 2-hydroxy group and compound activity. 2-Hydroxybenzyl derivative **B10** and 4-bromo-2-hydroxybenzyl **B18** exhibited similar activity at a concentration of 250 μM. Compounds

Downloaded from pubs.acs.org/amclct/article-pdf/17/9/1941/6469063/acsmedchemlett.6c00203.pdf by guest on 06 November 2026

https://doi.org/10.1021/acsmedchemlett.6c00203
ACS Med. Chem. Lett. 2026, 17, 1941−1947

containing fluorine and methyl group (**B23**−**B26**) demonstrated IC_{50} values in the range of 15−54 μM.

The closest analogue to compound **B19**, 2-hydroxy-4-methoxybenzyl derivative **B22**, showed 1 μM activity. The results for compounds **B23**−**B26** show that substitution at the 2,4-position of the benzene ring confers greater activity than substitution at the 2,5-positions relative to piperazine.

Potential modifications of the 2-hydroxy group were explored, leading to the synthesis of a carboxylic acid analogue **B27**, in which the carboxylate was expected to interact with the backbone of Asp169. However, no improvement in the activity was observed. Additionally, more bulky and less acidic 2-hydroxymethyl group-containing analogue **B28** and 2-methylamino-containing **B29** are less active than **B10**.

Next, we investigated some possible modifications of the piperazine and synthesized six compounds (**B30**−**B35**), where piperazine was replaced with structural analogues to assess how these changes affect biological activity. The inhibitory activity data indicate that piperazine can be replaced with 1,4-diazepane or hydroxypiperidine, as compounds **B32** and **B35** exhibited activity comparable to their respective analogues **B7** and **B12**. *p*-Benzonitrile aminopiperidine analogue **B34** outperformed the piperazine compound **B13**, improving the activity by more than 3-fold. Compound **B30**, which contains an additional carbonyl group, and aminoazetidine **B33** were less successful modifications, displaying reduced activity. The extended version of parent compound **B7**, aminopiperidine **B31**, lost its activity, indicating that the increased molecular size may hinder the binding.

To further investigate the influence of compound rigidity, we obtained adenosylpiperazine **B36** as a more flexible analogue of compound **B7**. The loss of the carbonyl group resulted in complete loss of activity, indicating that the amide bond in adenosine 5′-carboxamides is essential for maintaining the molecular geometry necessary for receptor interaction.

With the submicromolar inhibitor **B19** in hand, we decided to assess its selectivity and compare it with two other members of the series, namely, **B2**, whose selectivity had been measured in an early phase of this campaign, and **B22**. As in a previous study,[25] we selected a panel of SAM-dependent methyltransferases, including DOT1L, G9a, MLL4, PRDM9, PRMT1, SETD2, SMYD3, and METTL3/METTL14 (Table 2). At a concentration of 20 μM, **B2** and **B22** do not inhibit any of these methyltransferases. Compound **B19** showed weak inhibitory activity on histone lysine *N*-methyltransferases G9a and SETD2. These results suggest that the 5′-(*N*-piperazinylcarboxamido)-adenosine scaffold imparts selectivity for METTL1 compared to other methyltransferases.

Table 2. Methyltransferase Selectivity Measured by a Radiometric Assay[a]

methyltransferase	B2	B19	B22
DOT1L	94	97	79
G9a	101	**29**	107
MLL4 complex	96	80	99
PRDM9	107	93	104
PRMT1	93	101	102
SETD2	95	**39**	105
SMYD3	100	96	97
METTL3/METTL14	97	82	98

[a]remaining methyltransferase activity at 20 μM compound concentration,%. Values below 40% are in bold. Large values (above 75%) indicate lack of inhibition.

Kinetic solubility, mouse liver microsomal stability, and Caco-2 permeability were assessed for compounds **B2** and **B7** as part of an *in vitro* ADME early-stage profiling campaign (Table 3).

Table 3. Analysis of Physicochemical Properties, *in Vitro* Metabolic Stability, and Cellular Permeability[a]

				Caco-2 permeability, P_{app} (10^{-6} cm/s)		
compound	kinetic solubility,[b] μM	stability in PBS,[c] $T_{1/2}$, h	stability in mouse liver microsomes, $T_{1/2}$, min	A−B	B−A	efflux ratio
B2	437	29	>120	0.1	0.9	6.0
B7	382	n.d.	>120	0.2	0.7	3.2
B19	300	1	32.6[d]	n.d.	n.d.	n.d.
B22	447	10	239	n.d.	n.d.	n.d.

[a]n.d., not determined. [b]Target kinetic solubility 500 μM. [c]Stability was measured at 30 μM concentration at 37 °C. [d]Similar stability was observed in the assay without NADPH (Figure S5).

Compounds **B2** and **B7** exhibit high stability upon exposure to mouse liver microsomes and a favorable kinetic solubility. However, the Caco-2 assay indicates a very low intestinal absorption potential. The observed high metabolic stability of compounds **B2** and **B7** in microsomes may result from limited intracellular exposure and reduced access to hepatic metabolic enzymes. Compound **B19** showed reduced microsomal stability in the assay, both with and without NADPH. The half-life of **B19** in PBS buffer is 1 h. The low microsomal stability is likely due to its low chemical stability. As adenosine derivatives containing phenol groups, these compounds are very polar and may be susceptible to oxidation. Notably, the *p*-methoxy analogue **B22** shows high solubility, moderate stability in PBS, and a half-life of about 4 h in mouse liver microsomes.

In conclusion, a series of adenosine 5′-carboxamide derivatives were designed and synthesized starting from the hit compound **1**. Chemical modifications led to the identification of two potent METTL1 inhibitors: **B19** and **B22**. The benzylpiperazine moiety of the inhibitors is positioned in the RNA subpocket of METTL1 as revealed by the crystal structure of the METTL1/**B19** complex (PDB code 29GE). The positively charged piperazine ring is involved in favorable electrostatic interactions with the Glu210 side chain of the METTL1. The side chain of Asp169 forms a hydrogen bond with the hydrogen-bond-donating groups on the benzyl ring of **B19** (Figure 2A). These interactions provide a structural explanation for the high affinities of the top compounds. Our attempts to replace piperazine with other nitrogen-containing cycles suggest that piperazine in these structures may be replaced by diazepane (**B32**) or piperidine (**B34**). A selectivity analysis of three compounds of the series on a panel of eight methyltransferases provides evidence of selectivity for METTL1. Furthermore, **B22** shows favorable kinetic solubility and chemical and metabolic stability. Future work should aim at further increasing activity, stability, and cellular permeability.

Downloaded from pubs.acs.org/amclct/article-pdf/17/9/1941/6469063/acsmedchemlett.6c00203.pdf by guest on 06 November 2026

https://doi.org/10.1021/acsmedchemlett.6c00203
ACS Med. Chem. Lett. 2026, 17, 1941−1947

■ ASSOCIATED CONTENT

Supporting Information

The Supporting Information is available free of charge at https://pubs.acs.org/doi/10.1021/acsmedchemlett.6c00203.

Supplementary figures, table, experimental details of chemical synthesis and assays, crystallization procedure, data collection and refinement, description of docking studies (PDF)

NMR, HRMS and HPLC data for all final compounds (PDF)

■ AUTHOR INFORMATION

Corresponding Authors

Olga Bobileva − *Latvian Institute of Organic Synthesis, Riga LV1006, Latvia;* orcid.org/0000-0001-9600-1603; Email: olga_bobileva@osi.lv

Amedeo Caflisch − *Department of Biochemistry, University of Zurich, CH-8057 Zurich, Switzerland;* orcid.org/0000-0002-2317-6792; Email: caflisch@bioc.uzh.ch

Authors

Francesco Nai − *Department of Biochemistry, University of Zurich, CH-8057 Zurich, Switzerland;* orcid.org/0000-0002-4258-3174

Sandija Niedrite − *Latvian Institute of Organic Synthesis, Riga LV1006, Latvia*

Lidia Mayordomo Soler − *Department of Biochemistry, University of Zurich, CH-8057 Zurich, Switzerland*

Irena Leite − *Latvian Institute of Organic Synthesis, Riga LV1006, Latvia*

Complete contact information is available at: https://pubs.acs.org/10.1021/acsmedchemlett.6c00203

Author Contributions

The manuscript was written through contributions of all authors. All authors have given approval to the final version of the manuscript.

Notes

No unexpected or unusually high safety hazards were encountered.

The authors declare no competing financial interest.

■ ACKNOWLEDGMENTS

We thank Eduards Sevostjanovs and Baiba Gukalova for conducting the kinetic solubility assay, Maria Paula Flores Espinoza for biochemical experiments in an early phase of this work, and Pablo Andrés Vargas-Rosales for interesting discussions. The work was supported by Latvian Recovery and Resilience Grant No. 29/OSI/PG (No. 5.2.1.1.i.0/2/24/I/CFLA/001) (to O.B.) and Latvian Institute of Organic Synthesis Grant IG-2026-17 (to S.N.). The research group at the University of Zurich was supported by grants of the Lotte und Adolf Hotz-Sprenger Foundation and the Hartmann-Müller Foundation.

■ ABBREVIATIONS

HBTU, 2-(1*H*-benzotriazol-1-yl)-1,1,3,3-tetramethyluronium hexafluorophosphate; SAM, *S*-adenosylmethionine; SAH, *S*-adenosylhomocysteine; T3P, propanephosphonic acid anhydride

■ REFERENCES

(1) Santos-Pujol, E.; Quero-Dotor, C.; Esteller, M. Clinical Perspectives in Epitranscriptomics. *Curr. Opin. Genet. Dev.* **2024**, *87*, 102209.

(2) Li, J.; Wang, L.; Hahn, Q.; Nowak, R. P.; Viennet, T.; Orellana, E. A.; Roy Burman, S. S.; Yue, H.; Hunkeler, M.; Fontana, P.; Wu, H.; Arthanari, H.; Fischer, E. S.; Gregory, R. I. Structural Basis of Regulated M7G TRNA Modification by METTL1-WDR4. *Nature* **2023**, *613* (7943), 391−397.

(3) Ruiz-Arroyo, V. M.; Raj, R.; Babu, K.; Onolbaatar, O.; Roberts, P. H.; Nam, Y. Structures and Mechanisms of TRNA Methylation by METTL1-WDR4. *Nature* **2023**, *613* (7943), 383−390.

(4) Ranga, S.; Yadav, R.; Chauhan, M.; Chhabra, R.; Ahuja, P.; Balhara, N. Modifications of RNA in Cancer: A Comprehensive Review. *Mol. Biol. Rep.* **2025**, *52* (1), 321.

(5) Zhang, Y.; Xu, W.; Peng, C.; Ren, S.; Mustafe Hidig, S.; Zhang, C. Exploring the Role of M7G Modification in Cancer: Mechanisms, Regulatory Proteins, and Biomarker Potential. *Cell. Signal.* **2024**, *121* (July), 111288.

(6) Tian, Q.-H.; Zhang, M.-F.; Zeng, J.-S.; Luo, R.-G.; Wen, Y.; Chen, J.; Gan, L.-G.; Xiong, J.-P. METTL1 Overexpression Is Correlated with Poor Prognosis and Promotes Hepatocellular Carcinoma via PTEN. *J. Mol. Med.* **2019**, *97* (11), 1535−1545.

(7) Chen, Z.; Zhu, W.; Zhu, S.; Sun, K.; Liao, J.; Liu, H.; Dai, Z.; Han, H.; Ren, X.; Yang, Q.; Zheng, S.; Peng, B.; Peng, S.; Kuang, M.; Lin, S. METTL1 Promotes Hepatocarcinogenesis via M7G TRNA Modification-Dependent Translation Control. *Clin. Transl. Med.* **2021**, *11* (12), No. e661.

(8) Peng, W.; Fu, J.; Zhou, L.; Duan, H. METTL1/FOXM1 Promotes Lung Adenocarcinoma Progression and Gefitinib Resistance by Inhibiting PTPN13 Expression. *Cancer Med.* **2024**, *13* (13), No. e7420.

(9) Ying, X.; Liu, B.; Yuan, Z.; Huang, Y.; Chen, C.; Jiang, X.; Zhang, H.; Qi, D.; Yang, S.; Lin, S.; Luo, J.; Ji, W. METTL1-M7G-EGFR/EFEMP1 Axis Promotes the Bladder Cancer Development. *Clin. Transl. Med.* **2021**, *11* (12), No. e675.

(10) Dai, Z.; Liu, H.; Liao, J.; Huang, C.; Ren, X.; Zhu, W.; Zhu, S.; Peng, B.; Li, S.; Lai, J.; Liang, L.; Xu, L.; Peng, S.; Lin, S.; Kuang, M. N7-Methylguanosine TRNA Modification Enhances Oncogenic MRNA Translation and Promotes Intrahepatic Cholangiocarcinoma Progression. *Mol. Cell* **2021**, *81* (16), 3339−3355.

(11) García-Vílchez, R.; Añazco-Guenkova, A. M.; Dietmann, S.; López, J.; Morón-Calvente, V.; D'Ambrosi, S.; Nombela, P.; Zamacola, K.; Mendizabal, I.; García-Longarte, S.; Zabala-Letona, A.; Astobiza, I.; Fernández, S.; Paniagua, A.; Miguel-López, B.; Marchand, V.; Alonso-López, D.; Merkel, A.; García-Tuñón, I.; Ugalde-Olano, A.; Loizaga-Iriarte, A.; Lacasa-Viscasillas, I.; Unda, M.; Azkargorta, M.; Elortza, F.; Bárcena, L.; Gonzalez-Lopez, M.; Aransay, A. M.; Di Domenico, T.; Sánchez-Martín, M. A.; De Las Rivas, J.; Guil, S.; Motorin, Y.; Helm, M.; Pandolfi, P. P.; Carracedo, A.; Blanco, S. METTL1 Promotes Tumorigenesis through TRNA-Derived Fragment Biogenesis in Prostate Cancer. *Mol. Cancer* **2023**, *22* (1), 119.

(12) Ma, J.; Han, H.; Huang, Y.; Yang, C.; Zheng, S.; Cai, T.; Bi, J.; Huang, X.; Liu, R.; Huang, L.; Luo, Y.; Li, W.; Lin, S. METTL1/WDR4-Mediated M7G TRNA Modifications and M7G Codon Usage Promote MRNA Translation and Lung Cancer Progression. *Mol. Ther.* **2021**, *29* (12), 3422−3435.

(13) Xie, H.; Wang, M.; Yu, H.; Wang, H.; Ding, L.; Wang, R.; Luo, W.; Lu, Z.; Zheng, Q.; Ren, L.; Zhou, Z.; Su, W.; Xia, L.; Li, G. METTL1 Drives Tumor Progression of Bladder Cancer via Degrading ATF3 MRNA in an M7G-Modified MiR-760-Dependent Manner. *Cell Death Discovery 2022 81* **2022**, *8* (1), 1−14.

(14) Gao, Z.; Xu, J.; Zhang, Z.; Fan, Y.; Xue, H.; Guo, X.; Deng, L.; Wang, S.; Zhao, R.; Zhang, P.; Li, G. A Comprehensive Analysis of METTL1 to Immunity and Stemness in Pan-Cancer. *Front. Immunol.* **2022**, *13* (March), 1−15.

(15) Du, D.; Zhou, M.; Ju, C.; Yin, J.; Wang, C.; Xu, X.; Yang, Y.; Li, Y.; Cui, L.; Wang, Z.; Lei, Y.; Li, H.; He, F.; He, J. METTL1-Mediated TRNA M7G Methylation and Translational Dysfunction Restricts

Downloaded from pubs.acs.org/amclct/article-pdf/17/9/1941/6646906/acsmedchemlett.6c00203.pdf by guest on 06 November 2026

Breast Cancer Tumorigenesis by Fueling Cell Cycle Blockade. *J. Exp. Clin. Cancer Res. 2024 431* **2024**, *43* (1), 154.
(16) Ali, R. H.; Orellana, E. A.; Lee, S. H.; Chae, Y. C.; Chen, Y.; Clauwaert, J.; Kennedy, A. L.; Gutierrez, A. E.; Papke, D. J.; Valenzuela, M.; Silverman, B.; Falzetta, A.; Ficarro, S. B.; Marto, J. A.; Fletcher, C. D. M.; Perez-Atayde, A.; Alcindor, T.; Shimamura, A.; Prensner, J. R.; Gregory, R. I.; Gutierrez, A. A Methyltransferase-Independent Role for METTL1 in TRNA Aminoacylation and Oncogenic Transformation. *Mol. Cell* **2025**, *85* (5), 948−961.
(17) Ren, L.; Zhang, H.; Bobileva, O.; Nai, F.; Bi, H.; Baker, G.; Dong, L.; Guarin, D.; Chan, A.; Hu, W.; Li, W.; Leite, I.; Wang, X.; Zhang, X.; Xue, M.; Wang, H.; Qin, H.; Wu, X.; Ghoda, L.; Xu, L.; Zhang, B.; Li, L.; Wunderlich, M.; Mulloy, J.; Jones, C.; O'Leary, S.; Rosen, S.; Chen, C.-W.; Heisterkamp, N.; Perry, J. J.; Nam, Y.; Chen, J.; Li, X.; Caflisch, A.; Su, R. Targeting the METTL1/M7G Axis as a Therapeutic Strategy in Myeloid Leukemia. *Blood* **2025**, *146* (Supplement1), 2539−2539.
(18) Bowles, I. E.; Orellana, E. A. Rethinking RNA Modifications: Therapeutic Strategies for Targeting Dysregulated RNA. *J. Mol. Biol.* **2025**, *437* (16), 169046.
(19) Meidner, J. L.; Frey, A. F.; Zimmermann, R. A.; Sabin, M. O.; Nidoieva, Z.; Weldert, A. C.; Hoba, S. N.; Krone, M. W.; Barthels, F. Nanomole Scale Screening of Fluorescent RNA-Methyltransferase Probes Enables the Discovery of METTL1 Inhibitors. *Angew. Chem., Int. Ed.* **2024**, *63* (48), e202403792.
(20) Bucknell, S. J.; Thomas, E. J.; Brookfield, F. A.; Frost, L. M.; Bowles, L. J.; Mckee, S. T.; Martin, J. P.; Glen, A. Inhibitory Compounds. WO2025/104443, May 22, 2025.
(21) Nai, F.; Flores Espinoza, M. P.; Invernizzi, A.; Vargas-Rosales, P. A.; Bobileva, O.; Herok, M.; Caflisch, A. Small-Molecule Inhibitors of the M7G-RNA Writer METTL1. *ACS Bio Med. Chem. Au* **2024**, *4* (2), 100−110.
(22) Zhang, X.; Chen, Y.; Li, M.; Zhou, X.; Song, Q. METTL1 in Human Cancers: Recognition of Their Functions, Mechanisms and Therapeutic Value. *Oncol. Rev.* **2025**, *19*, 1637372.
(23) Epp, J. B.; Widlanski, T. S. Facile Preparation of Nucleoside-5'-Carboxylic Acids. *J. Org. Chem.* **1999**, *64* (1), 293−295.
(24) Dunker, C.; Schlegel, K.; Junker, A. Phenol (Bio)Isosteres in Drug Design and Development. *Arch. Pharm. (Weinheim)* **2025**, *358* (1), e2400700.
(25) Errani, F.; Invernizzi, A.; Herok, M.; Bochenkova, E.; Stamm, F.; Corbeski, I.; Romanucci, V.; Di Fabio, G.; Zálešák, F.; Caflisch, A. Proteolysis Targeting Chimera Degraders of the METTL3-14 M6A-RNA Methyltransferase. *JACS Au* **2024**, *4* (2), 713−729.

Downloaded from pubs.acs.org/amclct/article-pdf/17/9/1941/6469063/acsmedchemlett.6c00203.pdf by guest on 06 November 2026

https://doi.org/10.1021/acsmedchemlett.6c00203
ACS Med. Chem. Lett. 2026, 17, 1941−1947